Monthly Notices
of the
ROYAL ASTRONOMICAL SOCIETY

MNRAS **447,** 559–566 (2015) doi:10.1093/mnras/stu2454

Models of diffuse Hα in the interstellar medium: the relative contributions from *in situ* ionization and dust scattering

Joanna E. Barnes,[1⋆] Kenneth Wood,[1] Alex S. Hill[2†] and L. Matthew Haffner[3,4]

[1]*School of Physics & Astronomy, University of St Andrews, North Haugh, St Andrews, Fife, KY16 9SS, UK*
[2]*CSIRO Astronomy & Space Science, Marsfield, NSW 2122, Australia*
[3]*Department of Astronomy, University of Wisconsin Madison, 475 North Charter Street, Madison, WI 53706, USA*
[4]*Space Science Institute, 4750 Walnut Street, Suite 205, Boulder, CO 80301, USA*

Accepted 2014 November 17. Received 2014 October 21; in original form 2014 June 30

ABSTRACT

Using three-dimensional Monte Carlo radiation transfer models of photoionization and dust scattering, we explore different components of the widespread diffuse Hα emission observed in the interstellar medium of the Milky Way and other galaxies. We investigate the relative contributions of Hα from recombination emission in ionized gas and Hα that originates in H II regions near the Galactic mid-plane and scatters off high-altitude dust in the diffuse interstellar medium. For the radiation transfer simulations, we consider two geometries for the interstellar medium: a three-dimensional fractal geometry that reproduces the average density structure inferred for hydrogen in the Milky Way, and a density structure from a magnetohydrodynamic simulation of a supernova-driven turbulent interstellar medium. Although some sight lines that are close to H II regions can be dominated by scattered light, overall we find that less than ∼20 per cent of the total Hα intensity in our simulations can be attributed to dust scattering. Our findings on the relative contribution of scattered Hα are consistent with previous observational and theoretical analyses. We also investigate the relative contributions of dust scattering and *in situ* ionization of high-density dust clouds in the diffuse gas. Dust scattering in these partially ionized clouds contribute ∼40 per cent to the total intensity of Hα.

Key words: ISM: general – Galaxies: ISM.

1 INTRODUCTION

Widespread diffuse Hα emission is observed along all sight lines in the Milky Way and is ubiquitous in the interstellar medium (ISM) of other galaxies (see the extensive review by Haffner et al. 2009). The Hα intensity is attributed to recombination emission from diffuse ionized gas (DIG, also known as the warm ionized medium) in the ISM (e.g. Miller & Cox 1993; Dove & Shull 1994) with a contribution from Hα photons that originate in H II regions close to the Galactic mid-plane, and are scattered towards us by dust in the diffuse ISM (e.g. Jura 1979; Wood & Reynolds 1999). Power requirements for the DIG point to OB stars as the most likely source of its ionizing photons (e.g. Reynolds 1990). Observational and theoretical studies suggest that dust scattering is a relatively small component of the diffuse Hα emission, typically less than 20 per cent of the total.

Reynolds (1988) studied the [S II]/Hα optical line ratio and found it to be larger in the Galactic DIG than in H II regions. If scattered light were the dominant source of Hα and [S II] in the DIG then the line ratios would be similar to those observed in H II regions. In addition, observations of the DIG in the Milky Way and other galaxies show that line ratios of [S II]/Hα and [N II]/Hα increase with distance from the galactic mid-plane (e.g. Rand 1998; Haffner, Reynolds & Tufte 1999; Otte, Gallagher & Reynolds 2002; Hill et al. 2014). Observations of the Perseus Arm show that [S II]/Hα increases with decreasing Hα intensity (Haffner et al. 1999). In analysing recent observations of the Scutum–Centaurus Arm, Hill et al. (2014) found that the increase in the [S II]/Hα line ratios better correlate with decreasing Hα intensity than with height above the plane, suggesting that the trend in line ratios and accompanying changes in physical conditions are primarily a function of density, not the ionizing radiation field. The observed line ratios can be attributed to an increase in the temperature of the gas and has led to the suggestion that heating beyond that provided by photoionization is acting in the DIG (e.g. Bland-Hawthorn, Freeman & Quinn 1997; Reynolds, Haffner & Tufte 1999; Haffner et al. 2009).

Seon & Witt (2012) suggested that the elevated line ratios present in the ionized–neutral transition zone towards the edges of

⋆ E-mail: jb652@st-andrews.ac.uk
† Current address: Departments of Physics and Astronomy, Haverford College, Haverford, PA, USA.

H II regions could be responsible for the observed line ratios in the DIG, if dust scattering of light from H II regions was a large component of the DIG emission. However the transition zone comprises a very small component of the total emission from the H II region, so if dust scattering were dominant in the DIG we would expect H II region-like line ratios, as originally discussed by Reynolds (1988).

It has also been suggested that stellar Hα absorption lines are able to impact on observed emission lines, substantially increasing [S II]/Hα and [N II]/Hα line ratios in the DIG (Seon & Witt 2012). Other stellar absorption lines not coincident with ISM emission lines are also seen in WHAM (Wisconsin Hα Mapper) observations when the one-degree beam contains bright stars ($V < 7$ mag). However, these lines are not detectable in the ∼90 per cent of observations that contain only fainter sources, especially at moderate to high latitudes where diffuse stellar light is negligible. Further, Otte et al. (2001) and Otte et al. (2002) considered the effects of stellar absorption lines in edge-on galaxies and found no need for correction in DIG regions, only in those regions closer to the mid-plane. Finally, the scaleheight of stellar absorption and Hα emission are not comparable, and therefore, the effect of stellar absorption lines is unable to explain the observed increase with height in line ratios of [N II]/Hα and [S II]/Hα.

Using observations of the high-altitude cloud LDN 1780, Witt et al. (2010) derived a relation between the intensities of Hα and 100 μm thermal dust emission to estimate the dust-scattered Hα contribution. They extrapolated their results for the LDN 1780 cloud to the high-latitude ($|b| > 10^\circ$) sky to determine that the most probable scattered Hα intensity ($0.1R$[1]) is about 19 per cent of the most probable total Hα intensity in this portion of the sky ($0.52R$). This estimate for the dust-scattered Hα intensity agrees with estimates from Wood & Reynolds (1999), Reynolds, Scherb & Roesler (1973) and Brandt & Draine (2012).

From a theoretical perspective, Monte Carlo scattering simulations by Wood & Reynolds (1999) using a smooth ISM density structure (and assumed Hα emissivity from the DIG) found that less than 20 per cent of the total Hα intensity from the DIG is a result of dust-scattered Hα from H II regions. Their simulations showed spatial variations, with the scattered light component being smallest at high altitudes and with some sight lines towards the galactic mid-plane exhibiting a much larger scattered light component. The results from the smooth density ISM models of Wood & Reynolds (1999) are in broad agreement with other estimates of the dust-scattered contribution to the observed diffuse Hα (e.g. Reynolds 1988). If scattered light were a significant contributor to the observed Hα intensity it would complicate the interpretation of the observed Hα intensity as a tracer of the electron density along the line of sight. This would have significant implications for the understanding of both the energy transport in the ISM and for the use of Hα as a template for the Galactic foreground free–free contribution to the cosmic microwave background.

In this paper, we extend the work of Wood & Reynolds (1999) to study Hα emission and scattering in three-dimensional (3D) ISM density structures. Our models employ 3D Monte Carlo radiation transfer codes to compute the photoionization and temperature structure of the DIG and thus the 3D Hα emissivity from *in situ* recombinations. We then use a separate scattering code to compute the total intensity of Hα from *in situ* recombinations and Hα that originates in H II regions and is scattered by dust in the diffuse ISM. The setup of our simulations and methods are outlined in Section 2, our results are presented in Section 3, and our conclusions are presented in Section 4.

[1] $1\ R = 10^6/4\pi$ Hα photons cm^{-2} s^{-1} sr^{-1}.

2 MODELS

2.1 Photoionization models

For our study of photoionization and scattering in the DIG, we adopt two density structures. First, we consider a subsection of a supernova-driven, magnetohydrodynamic (MHD) simulation of the ISM that extends to $|z| = \pm 2$ kpc with width 1 kpc (Hill et al. 2012). The density in these simulations is strongly peaked around the mid-plane and has a small scaleheight, such that the density above ∼300 pc is smaller than inferred in the Galaxy. The MHD simulations include Type Ia and core-collapse supernovae set off at the average galactic supernova rate without knowledge of the gas distribution. They do not include photoionization; therefore, we post-process the density grids using our photoionization and scattered light codes.

Due to the small density scaleheight in the MHD simulations, we also consider a fractal density structure that has a vertical density distribution closer to that inferred for our Galaxy (Barnes et al. 2014). To create this model ISM we convert a smooth four-component density distribution to a fractal structure (see below). The smooth density comprises a Dickey–Lockman distribution (Dickey & Lockman 1990) plus an extended component:

$$n(z) = 0.4\mathrm{e}^{-(|z|/90)^2/2} + 0.11\mathrm{e}^{-(|z|/225)^2/2} + 0.06\mathrm{e}^{-|z|/400} + 0.04\mathrm{e}^{-|z|/1000}, \quad (1)$$

where the height z is in pc and number densities are in cm^{-3}.

When converted to a 3D fractal structure, this density is the input for our Monte Carlo photoionization and scattering simulations. The gas is initially assumed to be neutral and at the end of the photoionization simulations will comprise ionized and neutral components. The first three terms in equation (1) represent a Dickey–Lockman distribution for the average density of the neutral hydrogen. The fourth component is more vertically extended, and for fractal models is almost fully ionized at the end of our photoionization simulation, thus representing the density of the warm ionized medium with a 1 kpc scaleheight (Haffner et al. 1999).

To allow ionizing photons to propagate and reach gas at high altitudes, we convert the smooth structure to a fractal one using the algorithm of Elmegreen (1997) as described in Wood et al. (2005) where this algorithm has been scaled to the box size used here (1 kpc × 1 kpc × 4 kpc). We adopt a five-level clumping algorithm and arrange the density structure such that one-third of the mass is distributed smoothly, with the remainder in fractal clumps. The fractal algorithm maintains the total mass and average density with height. In both the smooth and fractal photoionization simulations, we begin by assuming all of the hydrogen is neutral, and then allow the gas to be ionized.

The resolution in both the MHD and fractal ISM models is 15.6 pc per grid cell, and we therefore do not resolve traditional parsec-scale H II regions around OB stars. We have investigated photoionization simulations with higher resolution and find there is little difference in the large-scale ionization and temperature structure between high- and low-resolution runs.

To determine the relative contribution of Hα from *in situ* recombination of ionized hydrogen in the DIG, we compute the 3D Hα emissivity using a Monte Carlo photoionization code (Wood, Mathis & Ercolano 2004). Due to the grid resolution described

above, the sources of ionizing radiation in our simulations represent photons escaping from H II regions. We reproduce the Galactic surface density of O stars in the solar neighbourhood (Garmany, Conti & Chiosi 1982) by randomly placing 24 sources in the xy plane with a scaleheight of 63 pc in $|z|$ (Maíz-Apellániz 2001). Since our simulations do not resolve the H II regions, we treat such regions as 'point sources' located at the source positions. In what follows, these sources will be referred to as 'H II regions'.

The spectrum of the sources in our ionization simulations is assumed to be that of a typical O star with $T = 35\,000$ K. Although altering the type of O star will lead to small changes in the temperature of the gas (and therefore the Hα emissivity) the most important variable is the ionizing luminosity (Wood et al. 2010).

We find from our ionization simulations that the ionizing luminosity that produces the extended DIG is $Q = 1 \times 10^{49}\,\mathrm{s}^{-1}$ for the MHD and $Q = 1.6 \times 10^{50}\,\mathrm{s}^{-1}$ for the fractal structure. Our photoionization code computes the gas temperature and ionization state of H, He, C, S, N, O and Ne in each cell. For an input density structure, we calculate the ionization and temperature structures arising from photoionization only, without considering photoelectric or shock heating, the two major heating mechanisms in the MHD simulations. The 3D Hα emissivity of the DIG then follows from our photoionized density grid.

Observations of ionized gas in other galaxies indicate that the Hα emission from the DIG is approximately equal to that from traditional H II regions (e.g. Ferguson et al. 1996; Zurita, Rozas & Beckman 2000; Thilker et al. 2002; Oey et al. 2007). We therefore calculate the Hα luminosity of the DIG in the photoionization simulations and set the Hα luminosity from the point sources equal to this. For the MHD simulations, the total Hα luminosity from H II regions, is $L_{\mathrm{H}\alpha} = 2.5 \times 10^{48}\,\mathrm{s}^{-1}$ and for the fractal simulations it is $L_{\mathrm{H}\alpha} = 6.5 \times 10^{49}\,\mathrm{s}^{-1}$. We adopt this approach for assigning the Hα luminosity from H II regions, but note that a fully self-consistent model would require subgrid resolution to compute the ionization structure and resulting Hα luminosity from the H II regions as well as the DIG.

The Hα emission in the DIG is a result of recombinations in the ionized gas. The number of Lyman continuum photons that can reach the DIG and ionize it depends on the number of photons that are able to escape H II regions and how many of these photons then escape the galaxy.

It is thought that globally 5 per cent of the Lyman continuum photons from OB stars escape the Galaxy (e.g. Barger, Haffner & Bland-Hawthorn 2013; Kim et al. 2013), 15 per cent produce the DIG (Reynolds 1990) and the remaining 80 per cent produce local H II regions close to sources. However, there is certainly local variation in these fractions, which we explore by varying the luminosity available to ionize the DIG versus H II regions. Rogers & Pittard (2013) used hydrodynamic models of massive star clusters to estimate that the percentage of ionizing photons that escape the cluster increases with age from 1 to 60 per cent over the first 4Myr of the cluster's evolution. Therefore, in addition to a model where the Hα flux from the DIG and H II regions are equal, we also investigate simulations where 30 per cent of the Hα flux originates in H II regions and 70 per cent in the DIG, and simulations where 70 per cent of the Hα flux originates in H II regions and 30 per cent in the DIG.

2.2 Scattered light models

To simulate the scattering of Hα photons we use the Monte Carlo scattering code described by Wood & Reynolds (1999). We assume that the dust and gas are well mixed and represented by a Mathis, Rumpl & Nordsieck (1977) mixture with total opacity $\kappa = 220\,\mathrm{cm}^2\,\mathrm{g}^{-1}$ and scattering albedo $a = 0.5$ appropriate for Hα photons. To describe the angular shape of the dust scattering we use a forward throwing Henyey–Greenstein phase function HG(θ) with anisotropy parameter $g = 0.44$,

$$\mathrm{HG}(\theta) = \frac{1}{4\pi}\frac{1-g^2}{(1+g^2-2g\cos\theta)^{3/2}}. \quad (2)$$

We use a 'forced first scattering' so every photon contributes to the scattered light intensity and a 'peeling off' algorithm forcing photons towards the observer with appropriate weights. We adopt the forced first scattering procedure to investigate scattered light in optically thin gas. Our scattered light models simulate the scattering of Hα photons that originate in both H II regions and the DIG.

3 RESULTS

The Monte Carlo scattering code computes the Hα intensity comprising photons that reach the observer without scattering from the DIG and point source H II regions. The code also computes the contributions from Hα photons that originate in the DIG and H II regions and are scattered into our line of sight. Therefore, there are four types of Hα photons present in our simulations as follows.

(i) Those that originate in H II regions and reach the observer without scattering.
(ii) Those that originate in H II regions and scatter off dust in the DIG before reaching the observer.
(iii) Those that originate in the DIG from recombinations and reach the observer without scattering.
(iv) Those that originate in the DIG from recombinations and scatter off dust before reaching the observer.

Because we wish to determine the relative contribution to the Hα intensity from photons that originate in H II regions and scatter in the DIG, we hereafter refer to case (ii) photons as 'scattered light' and photons in cases (iii) and (iv) as'diffuse'. We do not differentiate between Hα photons that originate in the DIG and reach the observer without scattering and those that originate in the DIG and are subsequently scattered.

3.1 Edge-on viewing

The upper panels of Fig. 1 show the total Hα intensity (photons that originate in the DIG plus those from H II regions including scattered photons) and the lower panels show the ratio of scattered to total intensity (photons from case (ii)/total Hα intensity). The fraction of scattered light appears to decrease with distance from the mid-plane; however, there are regions where the contribution from scattered light is large, particularly noticeable in the MHD simulations.

The fractal density structure (right-hand panels of Fig. 1) has a larger density scaleheight than that of the MHD simulations. This density structure is less centrally peaked than the MHD simulations and has higher density at large $|z|$ (see fig. 1 in Barnes et al. 2014). The right-hand panel of Fig. 1 shows maps of the total Hα intensity and the ratio of scattered to total intensity in a fractal density structure. Comparing the fractal models to the MHD density grid, we see that the total Hα intensity is higher above the mid-plane in the fractal models and the overall fraction of intensity that is dust scattered from H II regions is smaller.

The scattered light contribution to the total Hα emissivity scales as column density ($\sim n$) while the contribution from photoionization

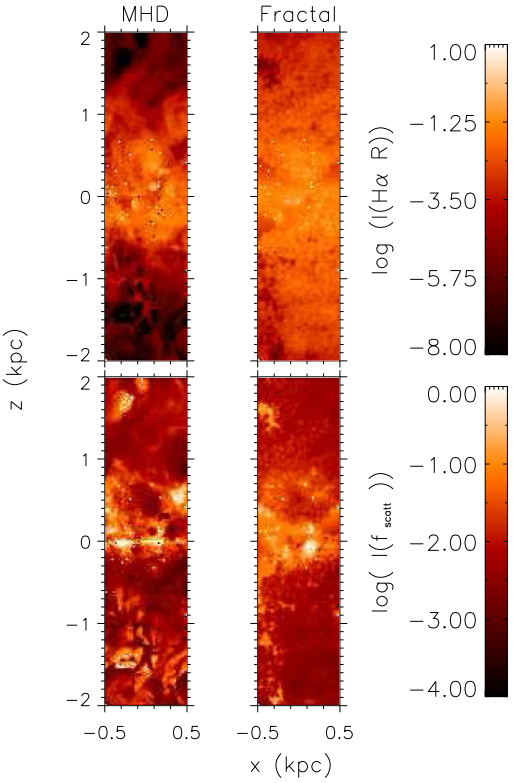

Figure 1. Maps showing total Hα intensity (top row) and fraction of scattered light that originates in H II regions (bottom row). Left: MHD simulations, right: fractal models using the HG scattering phase function.

scales as n^2. At low densities, dust scattering may therefore contribute a large fraction of the total Hα intensity. This results in the smaller fraction of scattered light in the fractal models.

Fig. 2 shows the fraction of scattered light intensity to total intensity for every 1-pixel-wide slice (grey lines) through the simulation box and the average fraction (black line). We find that on average the largest fraction (∼40 per cent) of scattered light is located close to the mid-plane of the simulation, where the density is highest. This is a result of the close proximity of the mid-plane dust to the H II regions and the $1/r^2$ dependence of scattered light. In the MHD simulations, the fraction of scattered light then decreases as the density decreases to below ∼10 per cent above $|z| \sim 300$ pc and below ∼5 per cent in the fractal models.

The large peaks in scattered light fraction above the mid-plane in the MHD simulations arise because of the very low density in individual cells resulting in low DIG emissivity. Since the DIG emissivity scales as $\sim n^2$ and scattered light scales as n, scattered light will dominate in these low-density cells. However in the MHD simulations, the total Hα intensity in the majority of the low-density regions is extremely faint and below the WHAM detection limit of $0.1R$.

Fig. 3 shows the total Hα intensity (black), intensity of Hα originating in the DIG (red) and intensity of dust-scattered Hα from H II regions (blue) for a 1-pixel-wide slice through the MHD and fractal simulations. The intensities of both the DIG and scattered light from H II regions peak close to the mid-plane of the simulation, where the density is highest and the dust is closest to the sources.

We have investigated models where we distribute the Hα luminosity such that 30 per cent of the total Hα flux originates in H II regions. The peak fraction of scattered light in these simulations decreases by between ∼10 and 20 per cent. If we distribute the Hα flux so 70 per cent originates in H II regions, then the peak fraction of scattered light increases by 10 per cent. In both cases the fraction

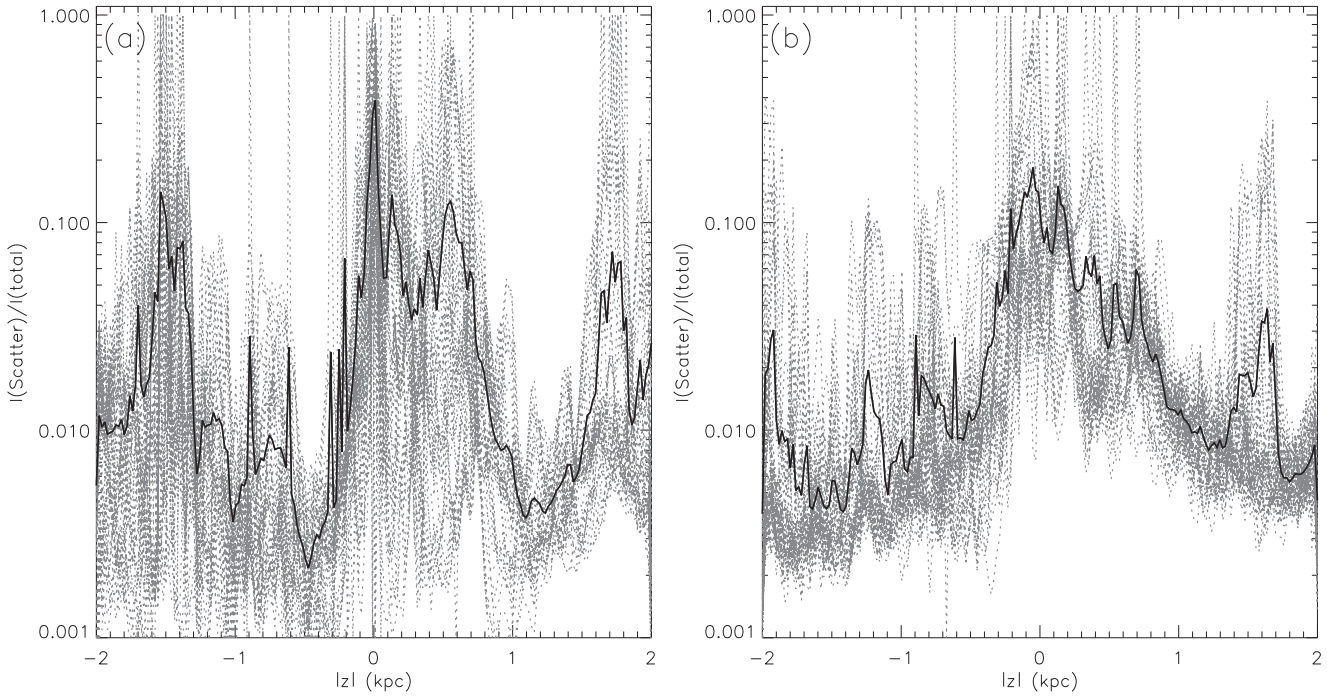

Figure 2. Ratio of scattered to total light versus distance from mid-plane. The solid line shows the average ratio and the dotted grey lines show every sight line through the simulations box for (a) MHD simulations, (b) fractal simulations with the HG phase function.

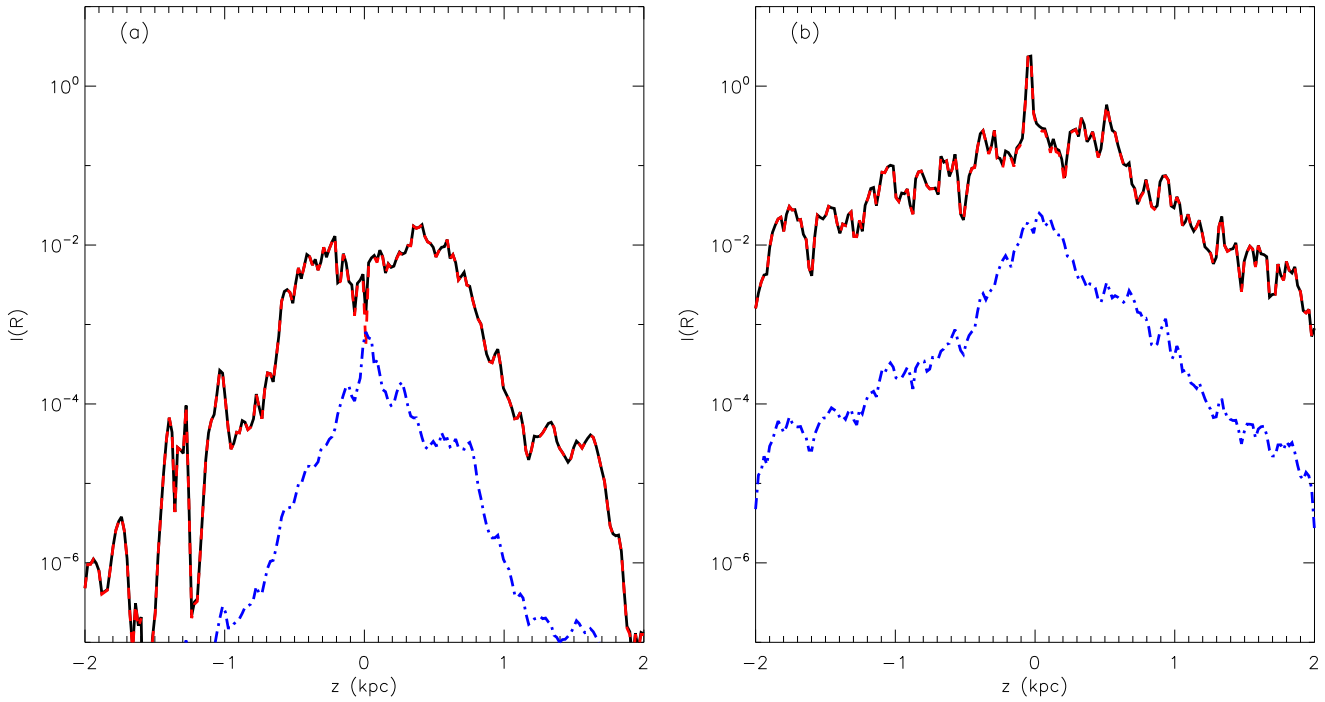

Figure 3. Intensity of total Hα (black), Hα in a 1-pixel-wide slice from photoionized DIG (red dashed), intensity of Hα from H II regions scattered in to the DIG (blue dot–dashed) for (a) MHD simulations, (b) fractal simulations with the HG phase function.

of scattered light still decreases to below ∼20 per cent in the MHD simulations. However, when the majority of the Hα flux originates in H II regions, the fraction of scattered light above the mid-plane increases to ∼10 per cent in the fractal models.

We have also investigated simulations using different albedo and scattering phase functions ($a = 0.67$, 0.77 and $g = 0.5$, 0.55 taken from Weingartner & Draine 2001). We find that altering the albedo and scattering phase function has qualitatively little effect on our simulations, with the greatest difference occurring when $a = 0.77$ and $g = 0.5$ where the fraction of scattered light is increased to ∼15 per cent above the mid-plane in MHD simulations. However, this does not significantly alter our results with the largest average fraction of scattered light increasing from 40 to 50 per cent.

3.2 Face-on viewing

Figs 4 and 5 show a face-on view of the Hα intensity of scattered light and the ratio of scattered light to total intensity. Face-on and edge-on viewing gives ratios of scattered to total Hα. Fig. 5 shows that in the MHD simulations the fraction of scattered light is typically below 20 per cent while it is below 10 per cent in the fractal models, consistent with our results from edge-on visualizations and with previous results (Reynolds 1988; Ferrara et al. 1996; Wood & Reynolds 1999)

3.3 Galactic cirrus

High-density clouds hundreds of parsecs above the mid-plane could have an effect on the fraction of total Hα intensity due to scattered light. Observations of the cloud LDN1780 led Witt et al. (2010) to determine that dust-scattered Hα accounts for ∼19 per cent of the Hα emission at high altitudes in the Galaxy. LDN 1780 is located approximate 110 pc above the mid-plane of the galaxy (Franco 1989), is approximately 1.2 pc in diameter and has an average density of $\sim 10^3$ cm^{-3}. To determine the contribution of dust-scattered light from such clouds, we estimate the thickness and Hα intensity of the ionized shell that results from photoionization using the following analysis. We assume a slab geometry for the cloud and plane parallel illumination.

The ionizing luminosity needed to ionize a volume δV is determined by

$$Q = n^2 \alpha_B \delta V \tag{3}$$

where Q is the number of ionizing photons per second incident on volume δV, n is the density of the gas (cm^{-3}), α_B is the recombination coefficient assuming Case B recombination. This can also be written in terms of the total ionizing flux available from O stars in the galaxy F_{LyC}:

$$F_{LyC} f \delta A = n^2 \alpha_B \delta A \delta l, \tag{4}$$

where δA is the area of the cloud exposed to the ionizing radiation, f is the fraction of ionizing photons that escape H II regions to produce the DIG and δl is the depth of the ionized volume in the cloud. Given an ionizing flux, the depth to which a cloud can be ionized is

$$\delta l = \frac{F_{LyC} f}{n^2 \alpha_B}. \tag{5}$$

The intensity of Hα emission in Rayleighs is related to the emission measure by

$$\mathrm{EM} = \int n^2 \mathrm{d}l = 2.75 T_4^{0.9} I_{H\alpha}(R)\ \mathrm{cm}^{-6}\ \mathrm{pc} \tag{6}$$

(Haffner et al. 1999). The Hα intensity can therefore be found using

$$I_{H\alpha}(R) = \frac{\int n^2 \mathrm{d}l}{2.75 T_4^{0.9}} \tag{7}$$

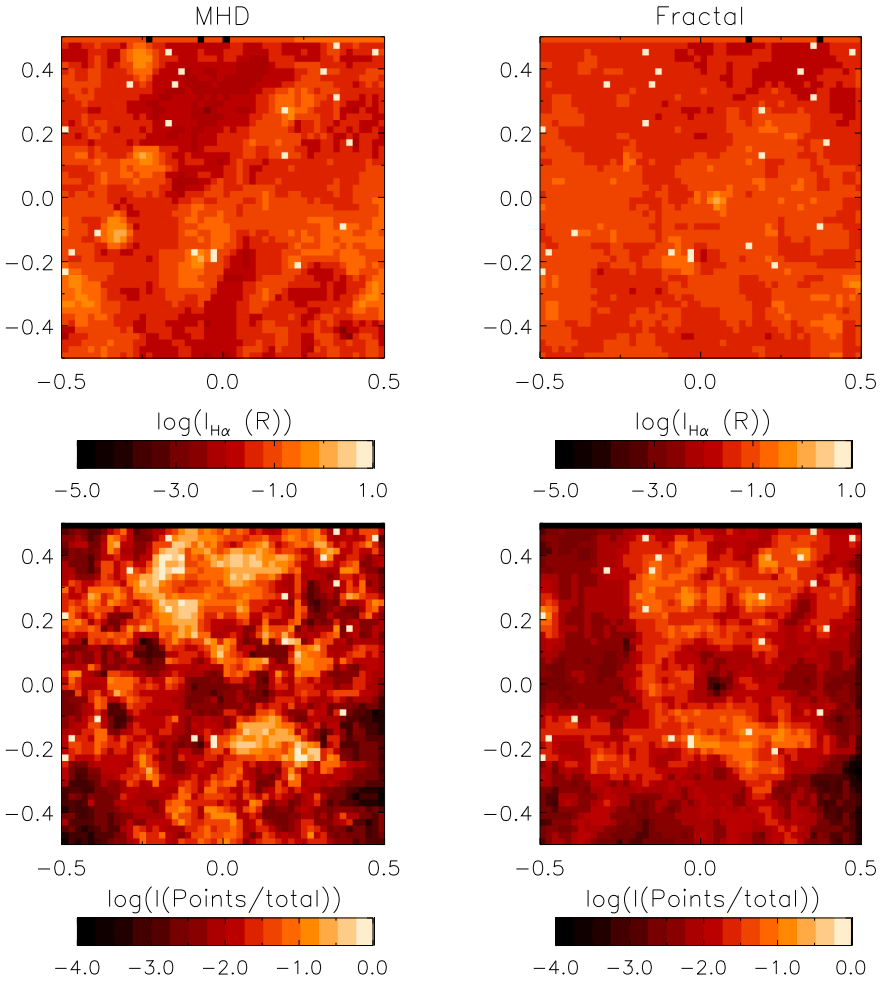

Figure 4. Maps showing total Hα intensity (top row) and fraction of scattered light that originates in H II regions (bottom row) for face-on views of our simulations. Left: MHD simulations and right: fractal simulations.

assuming the density is constant along the path dl this can be simplified to

$$I_{\mathrm{H}\alpha}(R) = \frac{n^2 \delta l}{2.75 T_4^{0.9}}, \tag{8}$$

where T_4 is the temperature of the gas in units of $T/10^4$ K and $I_{\mathrm{H}\alpha}$ is the intensity of Hα in Rayleighs (R).

Adopting $f = 0.15$, we would expect a cloud with density $n = 10^3\,\mathrm{cm}^{-3}$ and $T = 10^4$ K, ionized by the galactic ionizing flux from O stars, $F_{\mathrm{LyC}} = 3 \times 10^7\,\mathrm{cm}^{-2}\,\mathrm{s}^{-1}$(Reynolds et al. 1995), would be ionized to a depth of 6×10^{-6} pc and produce an Hα intensity of $2.2R$ from *in situ* recombinations.

Since we are unable to resolve an ionized skin of this thickness in the large-scale simulation presented in Section 2, we explore scattering on smaller scales with a model of a single cloud. The total Lyman continuum flux in the Galaxy is $3.74 \times 10^7\,\mathrm{cm}^{-2}\,\mathrm{s}^{-1}$ (Vacca, Garmany & Shull 1996). We assume that half of this flux travels upwards from the mid-plane of the Galaxy, towards the cirrus cloud, while the other half travels downwards, away from the cloud. We assume that 5 per cent of the Lyman continuum photons from each source escape the galaxy (e.g. Barger et al. 2013; Kim et al. 2013), 15 per cent produce the DIG (Reynolds 1990) and the remaining 80 per cent produce local H II regions around each source. We are considering the scattering of Hα photons that originate in H II regions, which are produced by 80 per cent of the total ionizing luminosity. Assuming Case B recombination, each Lyman continuum photon produces 0.46 Hα photons (Martin 1988). Therefore, the Hα flux impinging on galactic cirrus clouds is $0.46 \times 0.8 F_{\mathrm{LyC}} = 0.37 F_{\mathrm{LyC}} = 6.9 \times 10^6\,\mathrm{cm}^{-2}\,\mathrm{s}^{-1}$.

To determine the contribution of dust scattering in this cloud, we create simulations of a spherical cloud with $r = 0.5$ pc and $n = 10^3\,\mathrm{cm}^{-3}$ using a 200^3 pixel grid. The Hα flux incident on the cloud in this simulation is assumed to be directed upwards from H II regions close to the mid-plane of the Galaxy. We then run the scattered light simulations described above and find that the intensity of Hα scattered by the cloud is $1.4R$, which is about 40 per cent of the total Hα intensity from the cloud. These results indicate that the presence of high-density galactic cirrus can increase the contribution of dust-scattered light to the total Hα intensity we observe in the Galaxy. However, the intensity of Hα emission that results from ionization is still larger than that from scattering.

4 CONCLUSIONS

Using MHD and analytic fractal models for the 3D density structure appropriate for the ISM in the outer disc of a spiral galaxy, we have investigated the relative contributions to the Hα intensity from *in situ* recombinations of DIG and dust-scattered Hα originating in H II regions. Our models self consistently compute the diffuse

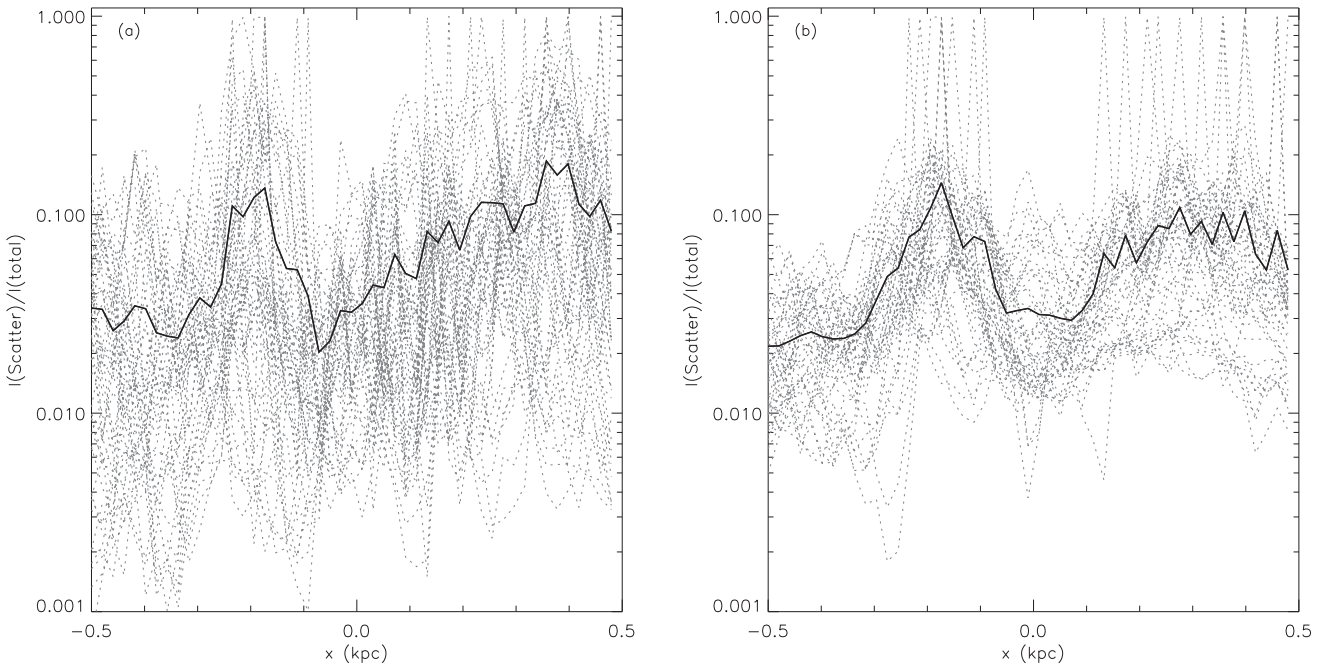

Figure 5. Face-on view of the ratio of scattered to total light versus distance from mid-plane. The solid line shows the average ratio and the dotted grey lines show every sight line through the simulations box for (a) MHD simulations and (b) fractal simulations with the HG phase function.

Hα emissivity from DIG. We do not resolve small-scale H II regions within our photoionization simulations, so make the assumption that the Hα luminosity from H II regions is equal to what we compute from the DIG. The main results of our combined photoionization and Hα-scattered light models are as follows.

(i) The intensity of scattered Hα originating from H II regions differs depending on the density structure. In both fractal and MHD structures, the intensity of scattered light peaks around the mid-plane of the simulation closest to the H II regions and where the gas density is highest. The intensity of scattered light then decreases away from the mid-plane to less than about ∼10 per cent in the MHD and ∼5 per cent in fractal models. The larger scattered light fraction in the MHD simulations is due to the very low densities and hence low intrinsic Hα emissivity at large heights in those models.

(ii) In low-density regions, a large fraction of the Hα in our simulations is dust-scattered light that originates in H II regions, a result of the small Hα emissivity from the lowest density DIG.

(iii) Different scattering phase functions and albedo affect the intensity of scattered light in the models; however, this does not significantly change our results, increasing the largest fraction of scattered light by 10 per cent.

(iv) Scattering of Hα photons from H II regions off high-density cirrus in the ISM can dominate over the Hα intensity from photoionization, contributing 40 per cent of the total Hα. However, the covering fraction of such clouds is ∼50 per cent (Gillmon & Shull 2006), so such clouds would not affect all sight lines through the Galaxy.

ACKNOWLEDGEMENTS

The authors would like to thank Kwang Il-Seon and Adolf Witt for their helpful comments on an early version manuscript. JB acknowledges the support of an STFC studentship. LMH acknowledges support from the US National Science Foundation through award AST-1108911.

REFERENCES

Barger K. A., Haffner L. M., Bland-Hawthorn J., 2013, ApJ, 771, 132
Barnes J. E., Wood K., Hill A. S., Haffner L. M., 2014, MNRAS, 440, 3027
Bland-Hawthorn J., Freeman K. C., Quinn P. J., 1997, ApJ, 490, 143
Brandt T. D., Draine B. T., 2012, ApJ, 744, 129
Dickey J. M., Lockman F. J., 1990, ARA&A, 28, 215
Dove J. B., Shull J. M., 1994, ApJ, 430, 222
Elmegreen B. G., 1997, ApJ, 477, 196
Ferguson A. M. N., Wyse R. F. G., Gallagher J. S., III, Hunter D. A., 1996, AJ, 111, 2265
Ferrara A., Bianchi S., Dettmar R.-J., Giovanardi C., 1996, ApJ, 467, L69
Franco G. A. P., 1989, A&A, 223, 313
Garmany C. D., Conti P. S., Chiosi C., 1982, ApJ, 263, 777
Gillmon K., Shull J. M., 2006, ApJ, 636, 908
Haffner L. M., Reynolds R. J., Tufte S. L., 1999, ApJ, 523, 223
Haffner L. M. et al., 2009, Rev. Mod. Phys., 81, 969
Hill A. S., Joung M. R., Mac Low M.-M., Benjamin R. A., Haffner L. M., Klingenberg C., Waagan K., 2012, ApJ, 750, 104
Hill A. S., Benjamin R. A., Haffner L. M., Gostisha M. C., Barger K. A., 2014, ApJ, 787, 106
Jura M., 1979, ApJ, 227, 798
Kim J.-h., Krumholz M. R., Wise J. H., Turk M. J., Goldbaum N. J., Abel T., 2013, ApJ, 775, 109
Maíz-Apellániz J., 2001, AJ, 121, 2737
Martin P. G., 1988, ApJS, 66, 125
Mathis J. S., Rumpl W., Nordsieck K. H., 1977, ApJ, 217, 425
Miller W. W., III, Cox D. P., 1993, ApJ, 417, 579
Oey M. S. et al., 2007, ApJ, 661, 801
Otte B., Reynolds R. J., Gallagher J. S., III, Ferguson A. M. N., 2001, ApJ, 560, 207
Otte B., Gallagher J. S., III, Reynolds R. J., 2002, ApJ, 572, 823
Rand R. J., 1998, ApJ, 501, 137
Reynolds R. J., 1988, ApJ, 333, 341

Reynolds R. J., 1990, ApJ, 349, L17
Reynolds R. J., Scherb F., Roesler F. L., 1973, ApJ, 185, 869
Reynolds R. J., Tufte S. L., Kung D. T., McCullough P. R., Heiles C., 1995, ApJ, 448, 715
Reynolds R. J., Haffner L. M., Tufte S. L., 1999, ApJ, 525, L21
Rogers H., Pittard J. M., 2013, MNRAS, 431, 1337
Seon K.-I., Witt A. N., 2012, ApJ, 758, 109
Thilker D. A., Walterbos R. A. M., Braun R., Hoopes C. G., 2002, AJ, 124, 3118
Vacca W. D., Garmany C. D., Shull J. M., 1996, ApJ, 460, 914
Weingartner J. C., Draine B. T., 2001, ApJS, 134, 263
Witt A. N., Gold B., Barnes F. S., III, DeRoo C. T., Vijh U. P., Madsen G. J., 2010, ApJ, 724, 1551
Wood K., Reynolds R. J., 1999, ApJ, 525, 799
Wood K., Mathis J. S., Ercolano B., 2004, MNRAS, 348, 1337
Wood K., Haffner L. M., Reynolds R. J., Mathis J. S., Madsen G., 2005, ApJ, 633, 295
Wood K., Hill A. S., Joung M. R., Mac Low M.-M., Benjamin R. A., Haffner L. M., Reynolds R. J., Madsen G. J., 2010, ApJ, 721, 1397
Zurita A., Rozas M., Beckman J. E., 2000, A&A, 363, 9

This paper has been typeset from a TEX/LATEX file prepared by the author.